Transient nutation signal locking

R. N. Shakhmuratov
Instituut voor Kern- en Stralingsfysica, Katholieke Universiteit Leuven, Celestijnenlaan 200 D, B-3001 Leuven, Belgium and Kazan Physical-Technical Institute, Russian Academy of Sciences, 10/7 Sibirsky Trakt Street, Kazan 420029, Russia
(Received 26 October 1998)

A method of making the dephasing time T_{2u} measurement in an ensemble of inhomogeneously broadened two-level systems is proposed. This method has its origin in the spin-locking technique developed in NMR. It is shown that in spite of inhomogeneous broadening it is possible to lock the induced polarization in phase with the driving field. The amplitude of the locked polarization can be as large as half of the first maximum of the nutation signal, i.e., of the polarization bump just after the pulse switch on. Decay of the locked polarization is caused by the T_{2u} dephasing or by the dephasing of the in-phase component of polarization.
[S1050-2947(99)08205-0]

PACS number(s): 42.50.Md, 76.60.Lz

I. INTRODUCTION

Ultrahigh resolution spectroscopy often encounters the problem of resolution of the absorption lines hidden by inhomogeneous scattering of their resonant frequencies. This problem is usually solved by pulse excitation. Different pulse sequences produce echo signals providing the information about absorption line structure and homogeneous broadening of line components. Steady state excitation has an effect on a homogeneous absorption line, resulting in saturation broadening, Mollow splitting [1–7], and dephasing suppression [8–14]. The last is attributed to the fast Rabi oscillations averaging the effect of the local fluctuating fields responsible for polarization decay. As the homogeneous absorption line is changed under the excitation, actual dephasing behavior of the driven polarization is of interest from the point of view, for example, of the hole burning study [12,15–21], of lasing without inversion [22–24], and of nonlinear interaction of the resonant fields with solids [25].

Dephasing of the driven polarization cannot be detected by a conventional echo inducing sequence. In its turn anomalous saturation seen in experiments [8–13] provides only indirect proof of the dephasing suppression as the saturated linewidth is sensitive to the ratio T_1/T_{2u}, where T_1 is a relaxation time of the population difference and T_{2u} is a homogeneous dephasing time of the u component of polarization, i.e., the component which is in phase with a driving field. Usually in solids T_1 is much longer than T_2, and when the ratio T_1/T_{2u} tends to 1 at elevated excitation, one can conclude that T_{2u} becomes as long as T_1.

Direct measurement of the dephasing time in pulse experiments [26,27] has demonstrated different results. Transient nutation decay [26] detected the increase of the dephasing rate with the increase of the driving field amplitude, whereas rotary echo [27] did not find any dependence on the field excitation.

However, both experiments detect the decay rate of the v component of the polarization, i.e., the component which is $\pi/2$ shifted relative to the driving field phase. Meanwhile, according to Redfield's theory of the spin temperature of the driven magnetization, only the $1/T_{2u}$ relaxation rate must change essentially as just this rate describes the energy exchange between spin system and thermal bath in the rotating reference frame [28]. Therefore it is interesting to consider another pulse scheme which could detect u-component decay having a strong effect on hole burning. For a nuclear spin system without inhomogeneous broadening this pulse sequence is known [29–31]. This is a spin-locking sequence making spin polarization in phase with a driving field. In Fig. 1(a) is shown the first stage of the spin locking when the resonant pulse of amplitude $\mathbf{H}_1$ and duration T turns the spin magnetization $\mathbf{M}_0$ around the x axis by an angle $\pi/2$. As a result the magnetization becomes parallel to the y axis. The x,y,z axes depict a rotating reference frame (RRF) chosen such that the circular polarized field $\mathbf{H}_1 \exp(i\omega t)$ (the field rotating around the z axis with the frequency ω) becomes constant [32]. The initial magnetization $\mathbf{M}_0$ is created by the

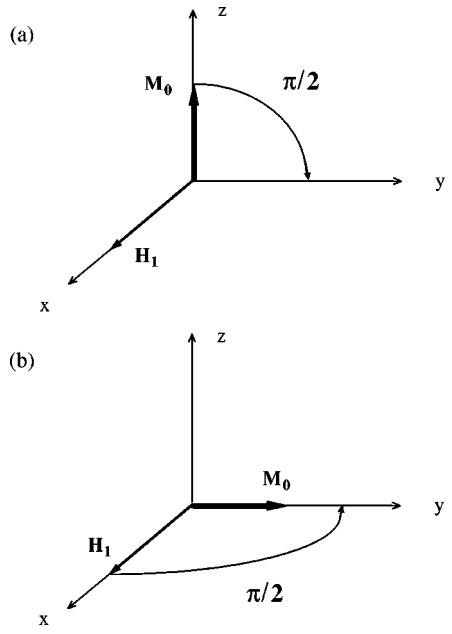

FIG. 1. (a) The first step of the spin-locking sequence when driving field $\mathbf{H}_1$ rotates the magnetization $\mathbf{M}_0$ around the x axis by an angle $\pi/2$. (b) The second step of the spin-locking sequence when the phase of the driving field has an abrupt $\pi/2$ phase shift to make the driving field and spin polarization in phase.

static magnetic field $\mathbf{H}_0$ which lies along the z axis. This field vanishes in RRF if the frequency of the driving field is equal to $\omega_0 = \gamma H_0/\hbar$, where γ is the gyromagnetic ratio. The energy $\hbar\omega_0$ is a spin splitting in the laboratory frame caused by $\mathbf{H}_0$. This splitting vanishes too in RRF.

At the second stage of the spin locking the driving field phase is shifted through an angle $\pi/2$ during very short time δt [see Fig. 1(b)]. Finally $\mathbf{H}_1$ lies along $\mathbf{M}_0$ and the latter will not nutate. Thus the magnetization is locked by the driving field. The field creates spin splitting γH_1 in RRF. Spin states separated by this splitting may come to equilibrium with environment only by the energy exchange. Therefore any dephasing process conserving the energy (for example, the part of the dipole-dipole interaction inducing flip-flop processes) cannot destroy the locked polarization $\mathbf{M}_0$ [28]. Moreover, if the energy scale of any other dephasing interaction not conserving the spin energy is smaller than the spin splitting then this dephasing cannot destroy the locked magnetization as well. This condition on the interaction energy scale or corresponding reservoir bandwidth is satisfied when the local field responsible for dephasing is smaller than H_1. At the mentioned condition the dephasing time T_{2u} of in-phase polarization becomes as long as T_1 [28]. While T_{2u} is no longer a dephasing time (as it is related to the energy exchange process in the RRF), the time T_{2v} is still related to the dephasing processes since it is a time of the coherence decay of the new spin states in the RRF as well as of the spin states in the laboratory frame. It is clearly seen from Fig. 1 where magnetization along the y axis corresponds to the coherence of the spin states split by the static magnetic field H_0 (parallel to the z axis) and this magnetization also represents the coherence of the spin states split by the field H_1 (parallel to the x axis).

The effect of the T_{2u} lengthening was employed by Hartmann and Hahn [30] in double nuclear magnetic resonance to increase the sensitivity of the method. It was tested with potassium chlorate, the sample in which potassium nuclei to be detected (either ^{39}K or ^{41}K) had ^{35}Cl nuclei as abundant neighbors yielding a large NMR signal. The dipole field due to the spins S (the potassium nuclei) determines a portion of the local field acting upon the spins I (the ^{35}Cl nuclei). If a radio-frequency pulse is applied to the spins S within the echo memory time T_2 of the spins I, the I echo is attenuated a certain amount because the local field due to the spins S is scrambled. The spin S resonance is therefore indicated. The sensitivity of this method increases when T_2 is effectively replaced by T_1 due to the magnetization locking in the rotating frame. Then during the time T_1 the spins S can be brought into resonance interaction with the spins I, after which a degradation in the magnetization of the I system is observed. Finally, it was shown that a minimum of 10^{14}–10^{16} nuclear Bohr magnetons/cm^3 could be detected in diamagnetic crystals in the temperature range of 4–20 K by this method.

For optical transitions the difference between T_{2u} and T_{2v} relaxation times has been discussed in paper [33].

When the absorption line is inhomogeneously broadened, the polarization of all spectral components cannot be aligned along the driving field amplitude simultaneously by any pulse sequence. Figure 2 shows two spectral components with different values of resonant detuning $\Delta = \omega_0 - \omega$, where

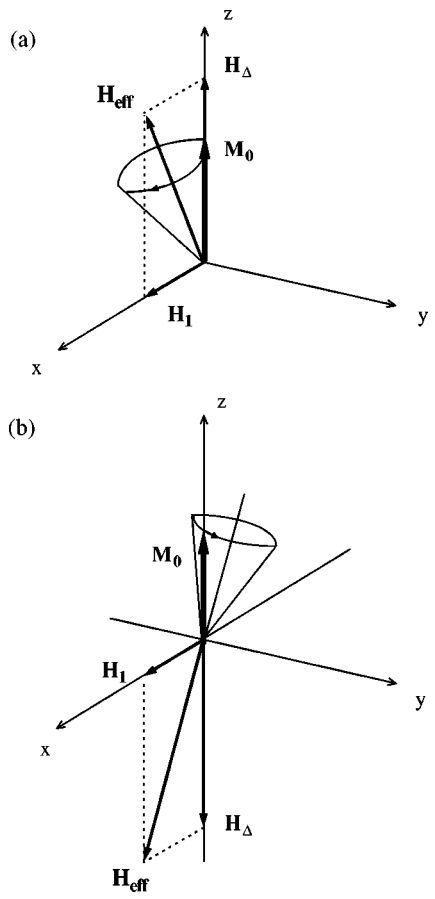

FIG. 2. Spin-precession picture at different detunings [positive (a) and negative (b)] in the rotating reference frame (RRF), where $H_\Delta = \gamma(\omega_0 - \omega)$ and $H_{\mathrm{eff}} = \sqrt{H_\Delta^2 + H_1^2}$.

$H_\Delta = \gamma\Delta$ is positive [Fig. 2(a)] and negative [Fig. 2(b)], and ω is a frequency of the driving field. Polarization nutates around the effective field $H_{\mathrm{eff}} = \sqrt{H_\Delta^2 + H_1^2}$ and depending on the sign of the tuning parameter its projection on the x axis is always positive or negative. Moreover, the maximum value of polarization projection on the y axis is smaller than M_0. Then spin locking of the resonant component $\Delta = 0$ does not stop the nutation of other components after the second stage. Nutation of these components on different frequencies H_{eff}/γ results in signal damping which is similar to transient nutation decay.

In this paper we show that this ringing on different frequencies does not decay to zero, in contrast to transient nutation. An appreciable part of the polarization does stop ringing with time and then decays with the rate $1/T_{2u}$. The amplitude of the locked signal can be as large as half of the the first bump of transient nutation signal

$$V_{\mathrm{TN}} = \sqrt{\frac{\pi}{2}}\frac{\chi}{\sigma}M_0,$$

where $\chi = \gamma H_1$ is Rabi frequency and σ is a dispersion of Gaussian inhomogeneous broadening.

So, inhomogeneous broadening does not prevent spin locking (SL) but only decreases it. This technique could help

to detect dephasing time T_{2u} during the excitation, the parameter which is important for hole burning and saturation studies.

II. SPIN DYNAMICS AT THE SPIN-LOCKING SEQUENCE

First we consider the solution of the Bloch equations

$$\dot{u}+\Delta v+u/T_{2u}=0, \tag{1}$$

$$\dot{v}-\Delta u-\chi w+v/T_{2v}=0, \tag{2}$$

$$\dot{w}+\chi v+(w-w_0)/T_1=0 \tag{3}$$

for the spin-locking sequence dropping the decay terms with T_{2u}, T_{2v}, T_1 relaxation times of u, v, w components. This solution helps to clarify spin dynamics at the SL sequence. In the next section we consider the kinetics of the locked polarization. Equations (1)–(3) follow from the density-matrix equations of motion for a two-level particle. The Bloch vector amplitudes u, v, and w are related to the density-matrix elements by $\rho_{12}=\frac{1}{2}(u+iv)e^{i\omega t}$, the dipole polarization term, and $\rho_{22}-\rho_{11}=w$, the population difference term. There is a correspondence between S_x, S_y, S_z spin components and u, v, w Bloch-vector components, respectively. Equilibrium population difference w_0 is related to the initial magnetization M_0.

(1) At the end of the first stage of the spin-locking sequence the pulse of the duration T changes the Bloch-vector components as follows:

$$u(T)=-\frac{w_0\Delta\chi}{g^2}(1-\cos gT), \tag{4}$$

$$v(T)=\frac{w_0\chi}{g}\sin gT, \tag{5}$$

$$w(T)=w_0\left[\left(\frac{\Delta}{g}\right)^2+\left(\frac{\chi}{g}\right)^2\cos gT\right], \tag{6}$$

where $g=\sqrt{\Delta^2+\chi^2}$. Here we assume the initial conditions $u(0)=v(0)=0$ and $w(0)=w_0$ before the excitation.

(2) At the second stage the field phase is turned through an angle $\pi/2$ during very short time δt, and as a result

$$u(T+\delta t)=v(T), \tag{7}$$

$$v(T+\delta t)=-u(T), \tag{8}$$

$$w(T+\delta t)=w(T). \tag{9}$$

We notice that by definition the u component is always in phase with the driving field and the v component is $\pi/2$ shifted.

(3) The evolution of the particle polarization after the phase shift is described by equations

$$u(t)=\frac{\Delta u(T)}{g}\sin gt+\frac{v(T)}{g^2}(\chi^2+\Delta^2\cos gt)$$

$$-\frac{\Delta\chi w(T)}{g^2}(1-\cos gt), \tag{10}$$

$$v(t)=[\Delta v(T)+\chi w(T)]\frac{\sin gt}{g}-u(T)\cos gt, \tag{11}$$

where time t is measured from the end of the phase shift.

For excitation at the center of a symmetric, inhomogeneous absorption line $f(\Delta)$, the average response of the particles

$$\langle u(t)\rangle=\int_{-\infty}^{\infty}u(\Delta,t)f(\Delta)d\Delta, \tag{12}$$

$$\langle v(t)\rangle=\int_{-\infty}^{\infty}v(\Delta,t)f(\Delta)d\Delta \tag{13}$$

has zero contribution of the odd components which are proportional to the functions $u(\Delta,T)$, $\Delta v(\Delta,T)$, and $\Delta w(\Delta,T)$. Then substitution of Eqs. (10) and (11) into Eqs. (12) and (13) gives the result

$$\langle u(t)\rangle=w_0f(0)[M_2(T)+M_2(t)-M_1(t)$$

$$-M_2(t+T)+M_1(t+T)], \tag{14}$$

$$\langle v(t)\rangle=w_0f(0)\left[M_1(t)-M_2(t)+\frac{1}{2}M_2(t+T)\right.$$

$$\left.+\frac{1}{2}M_2(t-T)\right], \tag{15}$$

where

$$M_k(t)=\int_{-\infty}^{\infty}\left(\frac{\chi}{g}\right)^{2k-1}\sin(gt)d\Delta \tag{16}$$

and the distribution $f(\Delta)$ is taken to be flat. The function $M_1(t)$ is well known (see, for example, [34]), i.e.,

$$M_1(t)=\pi\chi J_0(\chi t), \tag{17}$$

where $J_0(x)$ is a zeroth-order Bessel function. The second function $M_2(t)$ has been calculated and analyzed in Ref. [35]. This function can be expressed as follows:

$$M_2(t)=\pi\chi[\chi t-K(t)], \tag{18}$$

where

$$K(t)=\chi^2\int_0^t(t-\tau)J_0(\chi\tau)d\tau=\chi t[L(t)-J_1(\chi t)], \tag{19}$$

$$L(t)=\chi\int_0^t J_0(\chi\tau)d\tau \tag{20}$$

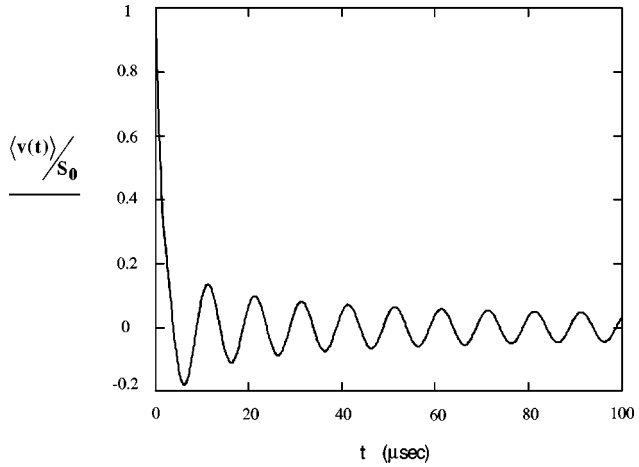

FIG. 3. Transient nutation decay of the averaged v component just after the spin-locking sequence terminated at time $t=0$, where $\chi/2\pi=100$ kHz as well as in the next plots below, $T=1.76$ μsec, and $S_0=\pi\chi f(0)w_0$.

and $J_1(x)$ is a first-order Bessel function. Finally, we get the expression for transient response of the system after the second stage of spin locking,

$$\langle u(t)\rangle=\pi\chi f(0)w_0[J_0(\chi(t+T))-J_0(\chi t)+K(t+T)-K(t)-K(T)], \tag{21}$$

$$\langle v(t)\rangle=\pi\chi f(0)w_0\left[J_0(\chi t)+K(t)-\frac{1}{2}K(t+T)-\frac{1}{2}\mathrm{sgn}(t-T)K(|t-T|)\right], \tag{22}$$

where $\mathrm{sgn}(t-T)$ is the sign of the difference $t-T$.

The mean value of the v component remarkably coincides with that which appears in rotary echo [36] and stimulated nutation echo [35]. Its dependence on time t and duration T of the preparative time interval was analyzed in detail in Refs. [35,36]. This component decays to zero with time. The example of its behavior is shown in Fig. 3. Figure 4 shows

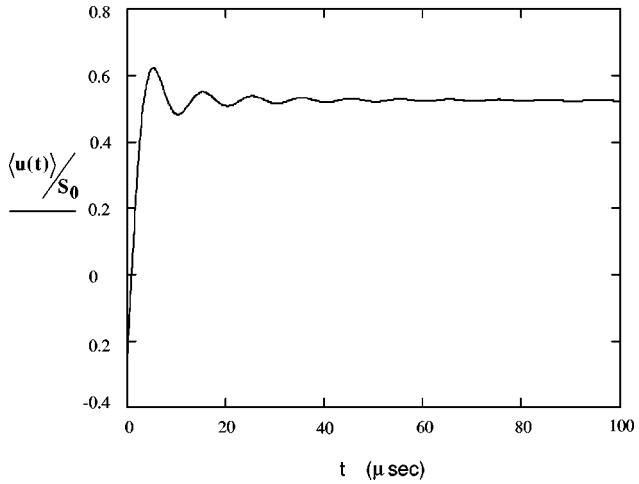

FIG. 4. Time evolution of the averaged u component just after spin-locking sequence. Parameters of excitation are the same as in Fig. 3.

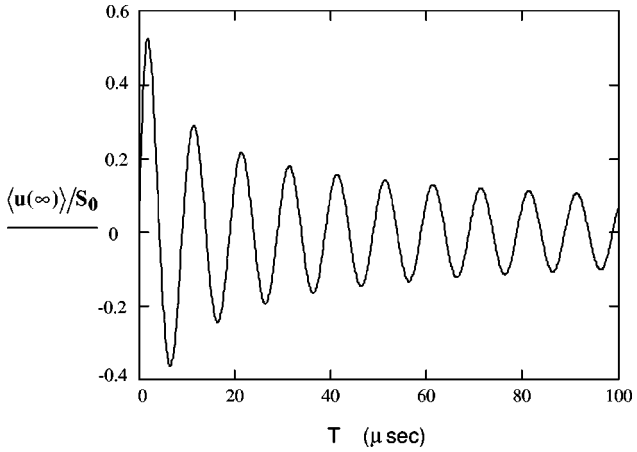

FIG. 5. The dependence of the locked polarization amplitude on the duration of the first preparative pulse T.

the time t dependence of the mean value of the u component (in all plots we take the same value of Rabi frequency $\chi/2\pi=100$ kHz as an example). It is seen that this component does not decay to zero. The value to which it tends is determined by the function

$$\langle u(\infty)\rangle=\pi\chi f(0)w_0[\chi T-K(T)] \tag{23}$$

since $J_0(\chi t)$ tends to zero with argument increase and other terms like $K(t+T)$ and $K(t)$ have asymptote

$$K(\tau)=\chi\tau+O_2(1/\sqrt{\chi\tau}) \tag{24}$$

at large $\chi\tau$, where $O_2(1/\sqrt{\chi\tau})$ is a small value of the order $1/\sqrt{\chi\tau}$ [35].

For the homogeneous system of the two-level particles it is possible to choose the length of the first stage T corresponding to the $(n+\frac{1}{2})\pi$ preparative pulse area when $\chi T=(n+\frac{1}{2})\pi$ and $n=0,1,2,\ldots$. After the $\pi/2$ phase shift of the driving field the polarization of the particles will be aligned along the field amplitude or opposite it depending on the parity of the number n. Pulses with even n (locking pulses) make polarization parallel and pulses with odd n (antilocking pulses) make it antiparallel to the driving field amplitude after the second stage ($n=0$ is supposed to be even).

When the absorption line is inhomogeneously broadened it is impossible to increase to infinity the preparative pulse area χT, as according to Eqs. (23) and (24) the locked polarization will decrease. Moreover, inhomogeneous broadening also changes the locking and antilocking pulse areas. They do not exactly equal $(n+\frac{1}{2})\pi$. Figure 5 shows the dependence of the locked polarization amplitude, Eq. (23), on preparing pulse duration. With T increase the locked polarization amplitude increases and then decreases with oscillations. First maximum

$$\langle u(\infty)\rangle_{\max}=\pi\chi f(0)w_0\times 0.524 \tag{25}$$

takes place when $\chi T=0.353\pi$, which is less than $\pi/2$. This maximum value is about half of the first nutation maximum after the simple pulse switch on. The minimum value of the antilocked signal is

$$\langle u(\infty)\rangle_{\min}=-\pi\chi f(0)w_0\times 0.364 \tag{26}$$

when $\chi T=1.293\pi$ (which is less than 1.5π too). These estimations show that inhomogeneous broadening does not prevent polarization locking.

The dependence of the function (23) on the preparing pulse area $\Theta=\chi T$ can be analyzed analytically as was done in Ref. [35]. The amplitude of the locked polarization reaches an extremum each time when the derivative of Eq. (23) with respect to pulse area Θ is equal to zero,

$$\langle u(\infty)\rangle'_{\Theta}=0. \tag{27}$$

The latter condition is reduced to

$$\langle u(\infty)\rangle'_{\Theta}=\pi\chi f(0)w_0[1-\mathcal{L}(\Theta)]=0, \tag{28}$$

where

$$\mathcal{L}(\Theta)=\int_0^{\Theta}J_0(x)dx.$$

The function $\mathcal{L}(\Theta)$ rises from 0 up to 1 almost linearly for $0\leqslant\Theta\leqslant 1$. The value 1 is reached at $\Theta\approx 1.108$. Then this function oscillates slightly near the value 1 with a damped amplitude. Therefore Eq. (28) becomes zero whenever $\mathcal{L}(\Theta)=1$. This occurs at $\Theta_1\approx 1.108$, $\Theta_2\approx 4.063$, $\Theta_3\approx 7.15$, etc. (see Ref. [34]). Maximum and minimum values of the locked polarization

$$\langle u(\infty)\rangle_{\mathrm{extr}}=\pi\chi f(0)w_0[\Theta_k-\mathcal{K}(\Theta_k)] \tag{29}$$

satisfy the equation

$$\langle u(\infty)\rangle_{\mathrm{extr}}=\pi\chi f(0)w_0\Theta_k J_1(\Theta_k), \tag{30}$$

where

$$\mathcal{K}(\Theta)=\int_0^{\Theta}(\Theta-x)J_0(x)dx$$

and Θ_k are the pulse areas when $\mathcal{L}(\Theta_k)=1$. Substitution, for example, $\Theta_1=1.1$ and $\Theta_2=4.05$ into Eq. (30), gives 0.52 V_{TN} and -0.36 V_{TN} values of the locked and antilocked polarizations, respectively, where V_{TN} is a first bump of the polarization in conventional transient nutation. With Θ_k increase, these extremum areas move to coincide with zeros of the $J_1(\Theta)$ function. Therefore the product $\Theta_k J_1(\Theta_k)$ tends to zero when Θ_k tends to infinity.

The experiment on spin locking is planned to be carried out with the equipment described in [26]. It detects the value

$$S(t)=\sqrt{\langle u(t)\rangle^2+\langle v(t)\rangle^2}, \tag{31}$$

the plot of which is shown in Fig. 6.

In the next section we consider the relaxation decay of the locked and antilocked polarization which takes place with the rate T_{2u}.

In the optical domain it is difficult to detect the u component directly. For example, the signal measured by the optical detector is induced mainly by v component. Therefore in order to detect the value of locked polarization it is useful to apply the unlocking procedure. For example, the next $\pi/2$ shift of the field phase converts the locked polarization $\langle u(+\infty)\rangle=\langle u_{\mathrm{loc}}\rangle$ into the v component. Then the nutation signal rises. By the value of the first nutation signal bump one can estimate the value of the locked polarization before the unlocking phase shift.

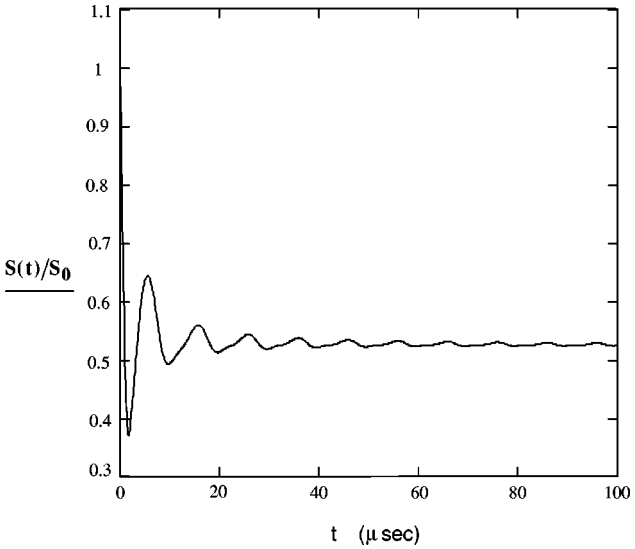

FIG. 6. Time evolution of the averaged polarization, Eq. (31), just after the spin-locking sequence with $T=1.76$ μsec.

Let us consider the case when the locking time interval between two phase shifts of the driving field is long enough to reach the nonoscillating state or $t=t_{\mathrm{loc}}$, where $\chi t_{\mathrm{loc}}\gg 1$. Just after the unlocking phase shift we have

$$v_{\mathrm{unloc}}(t)=\frac{\sin gt}{g}[\Delta u(0)+\chi w(0)]+v(0)\cos gt, \tag{32}$$

where t is measured after the second phase shift and

$$u(0)=v(t_{\mathrm{loc}}), \tag{33}$$

$$v(0)=-u(t_{\mathrm{loc}}), \tag{34}$$

$$w(0)=w(t_{\mathrm{loc}}) \tag{35}$$

are the initial conditions just after this phase shift. $u(t_{\mathrm{loc}})$ and $v(t_{\mathrm{loc}})$ components are described by Eqs. (10) and (11) where t is substituted by t_{loc} and

$$w(t_{\mathrm{loc}})=\frac{\chi u(T)}{g}\sin(gt_{\mathrm{loc}})-\frac{\Delta\chi v(T)}{g^2}[1-\cos(gt_{\mathrm{loc}})]$$

$$+\frac{w(T)}{g^2}[\Delta^2+\chi^2\cos(gt_{\mathrm{loc}})]. \tag{36}$$

Taking into account that odd terms in respect to the detuning Δ give zero contribution to the average response of the two-level particles as well as that $\chi t_{\mathrm{loc}}\gg 1$ and then the contribution of the oscillating terms as $\sin(gt_{\mathrm{loc}})$ and $\cos(gt_{\mathrm{loc}})$ is small one can obtain the average response

$$\langle v_{\mathrm{unloc}}(t)\rangle\simeq f(0)\int_{-\infty}^{\infty}v_{\mathrm{unloc}}(\Delta,t)d\Delta, \tag{37}$$

where

$$v_{\mathrm{unloc}}(\Delta,t)=w_0\frac{\chi}{g^3}\left\{[\Delta^2+\chi^2\cos(gT)]\left(\frac{\Delta}{g}\right)^2\sin(gt)\right.$$
$$\left.-\chi^2\sin(gT)\cos(gt)\right\}. \quad (38)$$

Equation (37) is reduced to

$$\langle v_{\mathrm{unloc}}(t)\rangle=f(0)w_0\left\{M_1(t)-2M_2(t)+M_3(t)+M_2(t-T)\right.$$
$$\left.-\frac{1}{2}[M_3(t+T)+M_3(t-T)]\right\}, \quad (39)$$

where

$$M_3(t)=\frac{\pi\chi^2 t}{6}\{[6-(\chi t)^2]J_1(\chi t)-\chi tJ_2(\chi t)+[3-(\chi t)^2]$$
$$\times[1-L(t)]\}$$

Just after the unlocking phase shift we have

$$\langle v_{\mathrm{unloc}}(+0)\rangle=f(0)w_0[\pi\chi-M_2(T)], \quad (40)$$

where

$$M_2(T)=\pi\chi[\Theta-\mathcal{K}(\Theta)]. \quad (41)$$

For the sequence with maximum polarization locking ($\Theta=\Theta_1$) the first bump of the nutation signal

$$\langle v_{\mathrm{unloc}}(+0)\rangle=f(0)w_0\pi\chi\times 0.48 \quad (42)$$

is two times smaller than its value just after the simple pulse switch on. Figure 7(a) shows the comparison of the nutation signal (39) at $\Theta=\Theta_1$ with the conventional nutation signal. When the locked polarization decays due to the T_{2u} irreversible dephasing process, then the term $M_2(T)$ decreases also and the $\langle v_{\mathrm{unloc}}(+0)\rangle$ value rises up to $f(0)w_0\pi\chi$.

The sequence resulting in antilocking ($\Theta=\Theta_2$) gives the first maximum of the nutation signal

$$\langle v_{\mathrm{unloc}}(+0)\rangle=f(0)w_0\pi\chi\times 1.36. \quad (43)$$

The comparison of Eq. (39) at $\Theta=\Theta_2$ with conventional nutation signal is shown in Fig. 7(b). In this case the relaxation process decreases the first nutation maximum. Figure 7(c) shows the nutation decay, Eq. (39), when the locking pulse area is $\Theta=\Theta_3$. As Θ_3 is big enough the last dependence demonstrates the signal near $t=T$ which is similar to the nutation echo.

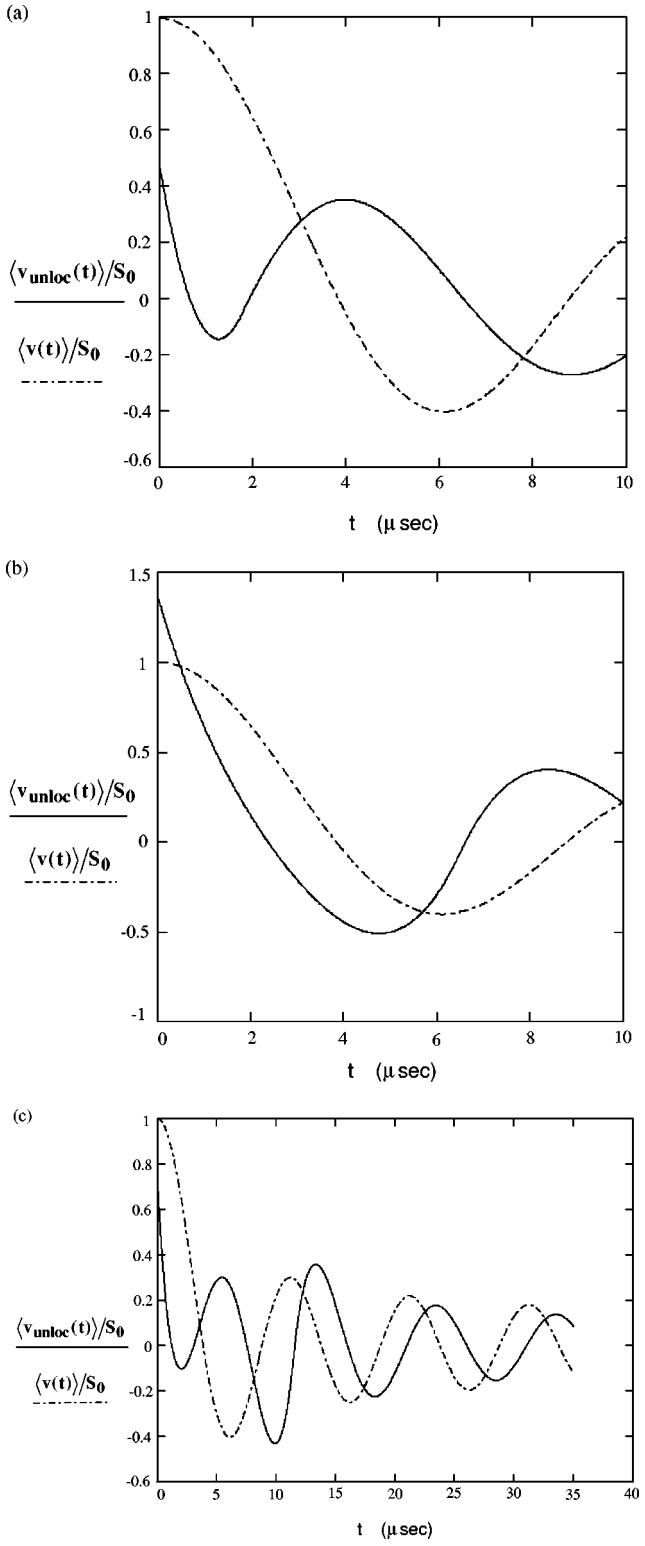

FIG. 7. Comparison of the conventional nutation signal (dashed-dotted line) with that induced by unlocking phase shift of the driving field (solid line). Preparative pulse areas are $\Theta=\Theta_1$ (a), $\Theta=\Theta_2$ (b), and $\Theta=\Theta_3$ (c), where $T=11.4$ μsec for case (c). Here $\langle v(t)\rangle$ is a conventional nutation signal after the pulse switches on.

III. KINETICS OF THE LOCKED POLARIZATION

Just after the phase shift of the driving field the transient signal appears (see Figs. 3, 4 and 6). It damps in a time scale of the order of $1/\chi$. Then only the locked component of polarization survives. The resonant frequency scattering does not destroy this component, which becomes time independent. On a time scale comparable to the relaxation times T_{2u} and T_{2v} the locked polarization will decay also. To simplify our consideration we study the relaxation of the locked polarization only. One can show that according to Eqs. (10) and (11) the locked part of the polarization comes from the $u(t)$ component and is proportional to $v(T)$ excited by the preparing pulse. Therefore we consider the $u(t)$ solution of Eqs.

(1)–(3) and only its part originated from $v(T)$ [i.e., the second term in the right hand side of Eq. (10)].

We assume that $T_1 \gg T_{2u}, T_{2v}$ and drop the population difference decay term in Eqs. (1)–(3). Solution of the Bloch equations is facilitated by application of the Laplace transform [37]

$$u(p)=\int_0^\infty u(t)e^{-pt}dt. \tag{44}$$

The mentioned part of $u(p)$ is

$$u_{\rm loc}(p)=\frac{v(T)}{D(p)}[p(p+\Gamma_v)+\chi^2], \tag{45}$$

where

$$D(p)=(p+\Gamma_u)[p(p+\Gamma_v)+\chi^2]+p\Delta^2 \tag{46}$$

and for the simplicity of the notations we use $\Gamma_u=1/T_{2u}$ and $\Gamma_v=1/T_{2v}$.

The solution of the equation $D(p)=0$ gives three poles of the Laplace transform (45) needed to calculate the inverse Laplace transform

$$u_{\rm loc}(t)=\frac{1}{2\pi i}\int_{c-i\infty}^{c+i\infty} e^{ipt}u_{\rm loc}(p)dp. \tag{47}$$

When $\Gamma_u=\Gamma_v=0$ they are

$$p_1=0, \quad p_{2,3}=\pm ig. \tag{48}$$

Application of the inverse Laplace transformation to Eq. (45) using poles (48) yields time dependent behavior

$$u_{\rm loc}(t)=\frac{v(T)}{g^2}(\chi^2+\Delta^2\cos gt) \tag{49}$$

[compare the latter with solution (10)]. Poles $p_{2,3}$ give the second, oscillating term in brackets, whereas the pole p_1 yields a nonoscillating term which corresponds to the locked polarization. We do not consider the oscillating part which decays due to ringing on different frequencies g. Thus, the true locked component originates from the pole p_1.

We consider the strong excitation when $\chi \gg \Gamma_u, \Gamma_u$. Then by iteration procedure we find

$$p_1 \simeq -\Gamma_u\left(\frac{\chi}{g}\right)^2 \tag{50}$$

and finally

$$u_{\rm loc}(t)\simeq\left(\frac{\chi}{g}\right)^3 w_0\sin(gT)\exp\left(-\Gamma_u\frac{\chi^2}{g^2}t\right). \tag{51}$$

The exact calculation of the average response (12) is rather complicated. When the preparing pulse area Θ is small ($\Theta \ll 1$), one can use the approximation

$$u_{\rm loc}(t)\simeq\left(\frac{\chi}{g}\right)^3 w_0 gT\exp\left(-\Gamma_u\frac{\chi^2}{g^2}t\right) \tag{52}$$

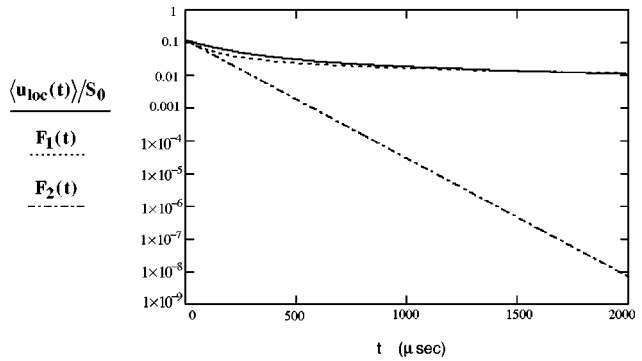

FIG. 8. Decay of the locked polarization. Solid line is a plot of the computer averaging of the $u_{\rm loc}(t)$ component. Dotted line is a plot of Eq. (53) normalized on S_0, i.e., $F_1(t)=S_1 I_0(t/2T_{2u})\exp(-t/2T_{2u})$, where $S_1=M_2(T)/(\pi\chi)$. Simple exponential decay $F_2(t)=S_1\exp(-t/T_{2u})$ (dashed-dotted line) is also presented for comparison. $T_{2u}=120$ μsec is taken as an example and $\Theta=0.125$.

as at large Δ ($|\Delta| \gg \chi$) $u_{\rm loc}(t)$ becomes small due to the fraction $(\chi/g)^3$. Then, one can calculate the integral (12) exactly,

$$\langle u_{\rm loc}(t)\rangle=\pi w_0 f(0)\chi\Theta I_0\left(\frac{\Gamma_u t}{2}\right)\exp\left(-\frac{\Gamma_u t}{2}\right), \tag{53}$$

where $I_0(x)$ is the modified Bessel function of zero order. The plots of the function (53) with computer calculation of the integral (12) at $\Theta=0.125$ are shown in Fig. 8 (in all plots below we take $T_{2u}=120$ μsec as an example). It is seen that the deviations between them are small. At long time ($\Gamma_u t \gg 1$) the function

$$I_0\left(\frac{\Gamma_u t}{2}\right)\exp\left(-\frac{\Gamma_u t}{2}\right) \tag{54}$$

approaches the asymptote

$$\frac{1}{\sqrt{\pi\Gamma_u t}}. \tag{55}$$

When preparative pulse area is large ($\Theta \gg 1$), one can use the expansion into a series

$$\langle u_{\rm loc}(t)\rangle=w_0 f(0)e^{-\Gamma_u t}\left[M_2(T)+\sum_{k=1}^{\infty}\frac{(\Gamma_u t)^k}{k!}N_k(T)\right], \tag{56}$$

where

$$N_k(T)=\int_{-\infty}^{\infty}\frac{\chi^3\Delta^{2k}}{g^{2k+3}}\sin(gT)d\Delta. \tag{57}$$

The integrals (57) are complicated, such as, for example, $N_1(T)=M_2(T)-M_3(T)$. However, any term of this expression can be calculated analytically using the relations

$$N_k(T)=\sum_{n=0}^{k}\frac{(-1)^n k!}{(k-n)!n!}M_{n+2}(T), \tag{58}$$

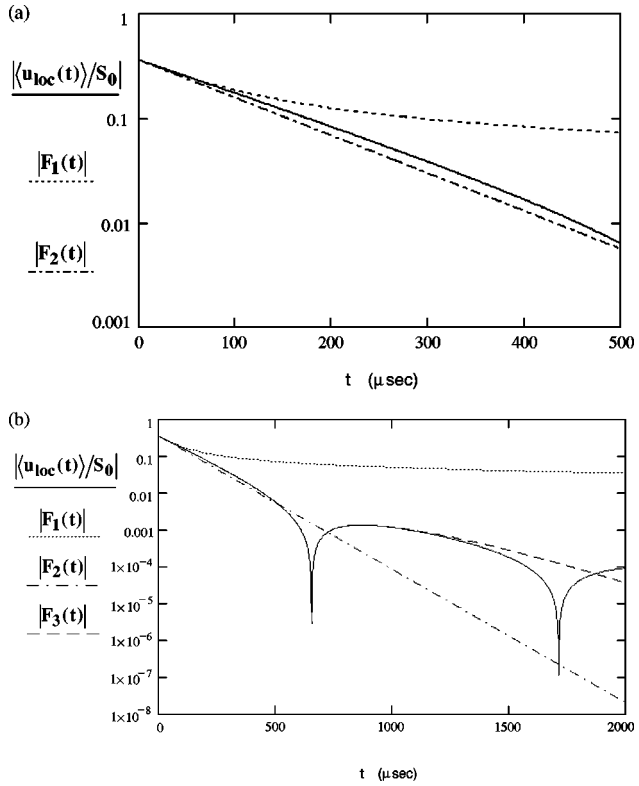

FIG. 9. Decay of the locked polarization at $\Theta=\Theta_2$. The notations are the same as in Fig. 8. Dashed line [in Fig. 9(b)] is a plot of the absolute value of Eq. (56), where the first ten terms of the expansion series are taken into account, i.e., it is a plot of $|F_3(t)| = |\langle u_{\rm loc}(t)\rangle/S_0|$, where $\langle u_{\rm loc}(t)\rangle$ is calculated from Eq. (56) at the mentioned condition.

$$M_n''(T) = -\chi^2 M_{n-1}(T), \tag{59}$$

where it is assumed that $0!=1$. Therefore the expression (56) can help only to estimate the value t when deviation from the exponential decay becomes pronounced. At the extremum pulse areas the first term of the expansion is

$$N_1\left(\frac{\Theta_k}{\chi}\right) = \pi\chi\frac{\Theta_k^2}{6}[J_2(\Theta_k)+\Theta_k J_1(\Theta_k)].$$

Figure 9 presents a numerical plot of average response (12) (absolute value) together with Eq. (56) (absolute value) where ten first terms of the expansion are taken into account (to have a coincidence with a second bump corresponding to the zero crossing it is necessary to take into account 20 terms). Pure exponential decay of the locked polarization is also presented. It is seen that the two order fall of the signal is close to the pure exponential one. Then the approximated calculation [when only the first term in square brackets of Eq. (56) is taken into account] diversifies the numerical result. Therefore one can use the first domain where the signal decreases 100 times to detect T_{2u} by simple fitting with exponent $\exp(-\Gamma_u t)$. The long time tail of the signal is not appropriate for this measurement because of nonexponential decay.

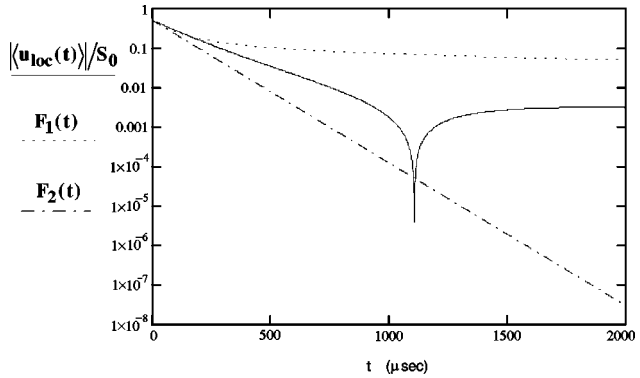

FIG. 10. Decay of the locked polarization at $\Theta=\Theta_1$.

It should be emphasized that when Θ is close to 1, this exponential fitting becomes poor (see Fig. 10). Therefore to measure T_{2u} one has to use the preparing pulse with the first antilocking pulse area $\Theta_2\approx 4$. In this case the locked signal is appreciably big and the fitting procedure of the decay function is simple. On the contrary, the first locking pulse area $\Theta_1\approx 1.1$ is too close to 1, giving the essential deviation from the exponential decay. In this case the fitting procedure is complicated and then T_{2u} measurement becomes obscure.

IV. CONCLUSION

We proposed a method of T_{2u} relaxation time measurement for the system of two-level particles with inhomogeneous broadening. The condition on the preparing pulse duration giving the best signal and providing the simple data analysis is derived. Experimental work is in progress.

ACKNOWLEDGMENTS

This work was supported by the IUAP Program IUAP P4-07, financed by the Belgian Federal Office for Scientific, Technical and Cultural Affairs, and by FWO, Vlaanderen and sponsored by the Research Fund K.U. Leuven.

[1] S. Autler and C.H. Towns, Phys. Rev. **100**, 703 (1955).
[2] S.G. Rautian and I.I. Sobel'man, Zh. Éksp. Teor. Fiz. **41**, 456 (1961) [Sov. Phys. JETP **14**, 328 (1962)].
[3] P.A. Apanasevich, Opt. Spektrosk. **14**, 612 (1963) [Opt. Spectrosc. **14**, 325 (1963)]; Bulletin of Belorussian Acad. Science **12**, 878 (1968) (in Russian).
[4] T.I. Kuznetsova and S.G. Rautian, Zh. Éksp. Teor. Fiz. **49**, 1605 (1965) [Sov. Phys. JETP **22**, 1098 (1966)].
[5] B.R. Mollow, Phys. Rev. A **5**, 2217 (1972).
[6] A.M. Bonch-Bruevich, V.A. Khodovoi, and N.A. Chigir', Zh. Éksp. Teor. Fiz. **67**, 2069 (1974) [Sov. Phys. JETP **40**, 1027 (1974)].
[7] F.Y. Wu, S. Ezekiel, M. Durkloy, and B.R. Mollow, Phys. Rev. Lett. **38**, 1077 (1977).
[8] R.G. DeVoe and R.G. Brewer, Phys. Rev. Lett. **50**, 1269 (1983).
[9] R. Boscaino, F.M. Gelardi, and G. Messina, Phys. Rev. A **28**, 495 (1983).

[10] A. Szabo and T. Muramoto, Phys. Rev. A **39**, 3992 (1989).
[11] R. Boscaino and V.N. La Bella, Phys. Rev. A **41**, 5171 (1990).
[12] A. Szabo and R. Kaarli, Phys. Rev. B **44**, 12 307 (1991).
[13] R. Boscaino and F.M. Gelardi, Phys. Rev. A **45**, 546 (1992).
[14] R.N. Shakhmuratov and A. Szabo, Phys. Rev. B **48**, 6903 (1993).
[15] R.N. Shakhmuratov and A. Szabo, Laser Phys. **3**, 1042 (1993).
[16] T. Endo, T. Muramoto, and T. Hashi, Opt. Commun. **51**, 163 (1984).
[17] A. Schenzle, M. Mitsunaga, R.G. DeVoe, and R.G. Brewer, Phys. Rev. A **30**, 325 (1984).
[18] P.R. Berman and R.G. Brewer, Phys. Rev. A **32**, 2784 (1985).
[19] M. Jamanoi and J.H. Eberly, Phys. Rev. Lett. **52**, 1353 (1984).
[20] K. Wodkiewicz and J.H. Eberly, Phys. Rev. A **32**, 992 (1985).
[21] R.N. Shakhmuratov, F.M. Gelardi, and M. Cannas, Phys. Rev. Lett. **79**, 2963 (1997).
[22] R.N. Shakhmuratov, Phys. Lett. **110A**, 379 (1985); Opt. Spektrosk. **58**, 568 (1985) [Opt. Spectrosc. **58**, 930 (1985)].
[23] R.N. Shakhmuratov, Kvant. Elektron. (Moscow) **13**, 271 (1986) [Sov. J. Quantum Electron. **16**, 182 (1986)].
[24] R.N. Shakhmuratov, Hyperfine Interact. **107**, 205 (1997).
[25] R.N. Shakhmuratov and R.A. Khasanshin, Opt. Commun. **124**, 263 (1996); Opt. Spectrosk. **79**, 370 (1995) [Opt. Spectrosc. **79**, 340 (1995)]; Proc. SPIE **3239**, 357 (1997).
[26] R. Boscaino, F.M. Gelardi, and J.P. Korb, Phys. Rev. B **48**, 7077 (1993).
[27] T. Muramoto and A. Szabo, Phys. Rev. A **38**, 5928 (1988).
[28] A.G. Redfield, Phys. Rev. **98**, 1787 (1955).
[29] I. Solomon, C.R. Hebd. Seances Acad. Sci. **248**, 92 (1959).
[30] S.R. Hartmann and E.L. Hahn, Phys. Rev. **128**, 2042 (1962).
[31] *Spin Temperature and Nuclear Magnetic Resonance in Solids*, edited by M. Goldman (Clarendon, Oxford, 1970).
[32] A. Abragam, *The Principles of Nuclear Magnetism* (Clarendon Press, Oxford, 1961).
[33] A.R. Kessel, R.N. Shakhmuratov, and L.D. Eskin, Zh. Éksp. Teor. Fiz. **94**, 202 (1988) [Sov. Phys. JETP **67**, 2071 (1988)].
[34] *Handbook of Mathematical Functions*, Natl. Bur. Stand. Appl. Math. Ser. No. 55, edited by M. Abramowitz and I.A. Stegun (U.S. GPO, Washington, DC, 1964).
[35] A. Szabo and R.N. Shakhmuratov, Phys. Rev. A **55**, 1423 (1997).
[36] N.C. Wong, S.S. Kano, and R.G. Brewer, Phys. Rev. A **21**, 260 (1980).
[37] A. Schenzle and R.G. Brewer, Phys. Rev. A **14**, 1756 (1976).